Interdiffusivity in Titanium–Tantalum Alloys Processed at 1473 K

by

Jennifer C. Dibbern

Submitted to the Department of Materials Science and Engineering
in partial fulfillment of the requirements for the degree of

Bachelor of Science

at the

MASSACHUSETTS INSTITUTE OF TECHNOLOGY

June 2007

Author .....
Department of Materials Science and Engineering
May 24, 2007

Certified by .....
Samuel M. Allen
POSCO Professor of Physical Metallurgy
Thesis Supervisor

Accepted by .....
Caroline A. Ross
Chair of the Undergraduate Committee

Interdiffusivity in Titanium–Tantalum Alloys Processed at 1473 K

by

Jennifer C. Dibbern

Submitted to the Department of Materials Science and Engineering
on May 24, 2007, in partial fulfillment of the
requirements for the degree of
Bachelor of Science

Abstract

Titanium–tantalum (Ti–Ta) alloys are likely to have a high biocompatibility and corrosion resistance that renders them novel materials of interest for biomedical applications[7, 14, 2]. With high strength and a low elastic modulus, Ti–Ta alloys have attracted attention as candidates for such uses as hip replacements[2]. A current challenge impeding use of these alloys is that, with a melting temperature of 3269 K, homogeneous alloys involving Ta are difficult to produce by conventional melting practice[3]. The objective of this work was to, as most structural changes occur via diffusion, gain insight into this matter through determination of the interdiffusivity in Ti–Ta alloys. A scanning electron microscope was utilized to perform energy dispersive x-ray analysis on Ti–Ta alloy samples in the range of 20 to 60 weight percent (wt %) Ta. A computational model that employed Fick's Second Law was used to extract interdiffusivity values from the data. Interdiffusivity values, which ranged from $4.0 \cdot 10^{-13} \frac{m^2}{s}$ for 20 wt % Ta to $3.0 \cdot 10^{-14} \frac{m^2}{s}$ for 60 wt % Ta, exhibited a systematic variation with composition. The interdiffusion coefficient was seen to decrease with increasing weight fraction Ta.

Thesis Supervisor: Samuel M. Allen
Title: POSCO Professor of Physical Metallurgy

Contents

List of Figures

Acknowledgments

There were many people who provided support and encouragment throughout the duration of this work. I would like to extend my appreciation and thanks to those who were always ready to offer assistance or advice–Professor Heather Lechtman, Dr. Tony Garratt-Reed, Yin-Lin Xie, and Donald Galler. I wish to express my gratitude to Professor Samuel Allen for his kind mentorship and advising. To my family and Josue Martinez I owe a special thanks for their unconditional support throughout this project and the past four years.

Chapter 1

Introduction

1.1 Background and Motivation

Titanium–tantalum (Ti–Ta) alloys combine four properties found infrequently together–biocompatibility, corrosion resistance, high strength, and low modulus (figure 1.1)[3, 10]. The coincidence of these qualities has sparked interest in Ti–Ta alloys for their possible utility in biomedical applications. With an elastic modulus lower and closer to that of bone, as compared to materials currently in use, specific compositions of Ti–Ta alloys have excellent potential for use as hip replacements (figure 1.1)[2, 3]. Interest in this materials system is augmented by the possibility of shape memory or superelastic behavior that is suggested by the presence of an observed martensite transformation in some compositions[8, 9, 10, 11]. Researchers continually seek novel shape memory materials for use in arenas such as arterial stents. There are, however, current challenges impeding further development and use of these alloys. One of the most fundamental and significant problems posed by these alloys is processing. Ta, as a refractory material, inhibits facile processing of these alloys[12, 15]. The significant difference in the molecular weights and atomic radii of Ti and Ta also make interdiffusion, a primary mechanism of structural changes, difficult and slow[1, 13]. Complications, such as those described by the Kirkendall effect, make processing Ti–Ta alloys to full density and homogeneity a unique challenge[1, 12, 13].

Quantification of the diffusion kinetics, specifically a measure of the interdiffusivity in Ti–Ta alloys, is necessary to address the processing quandries and dilemmas. Elucidation of the optimal homogenization treatments for Ti–Ta alloys is a direct application of such a result. While the processing history of a material can affect its measurable properties, determination of the interdiffusion

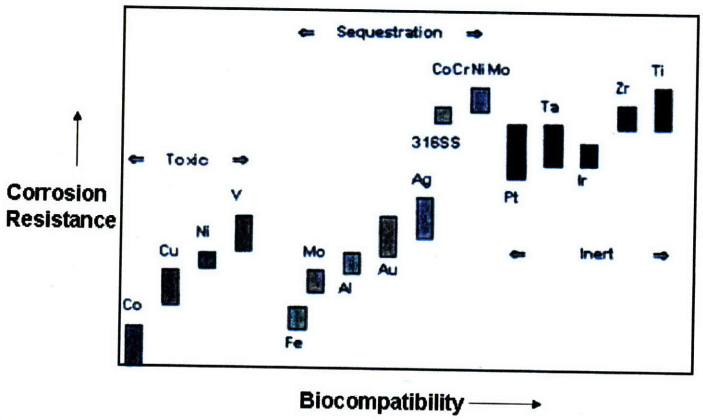

Figure 1-1: Biocompatability and corrosion resistance for different materials. Image courtesy of Dynamet.

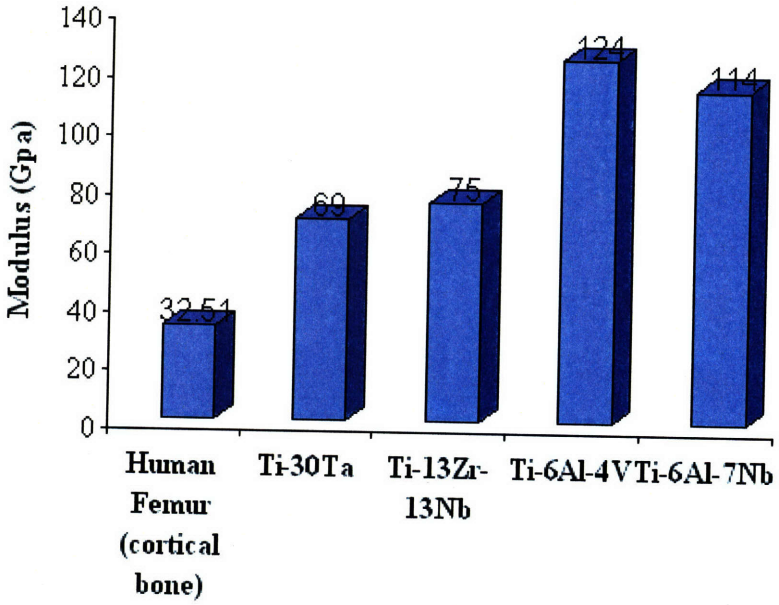

Figure 1-2: Chart of modulus values for Ti alloys used biomedically.

coefficient for Ti–Ta alloys as a function of composition should be a broadly applicable result. A diffusion coefficient is an intensive materials property that is proportional to the velocity of the diffusing particles and is, therefore, influenced by system temperature. Interdiffusion coefficients are the compositionally weighted average of the diffusion coefficients for each constituent element in an alloy. Feasible applications of this work are numerous as it provides information regarding a basic property of this materials system.

1.2 Objectives

The objective of this work was to compute the interdiffusion coefficients for Ti–Ta alloys through, in step compositions of 5 wt %, the range of 20 to 60 wt % Ta. Both experimental and computational modeling techniques were employed during the course of this investigation. A scanning electron microscope (SEM) was used to perform energy dispersive x-ray (EDX) analysis of each sample. Linear compositional traces, or linescans, were collected from each composition. From these linescans, data regarding compositional variance across the sample surface was obtained. These results were computationally modeled using a linearized Fick's Second Law to derive interdiffusivity values and ascertain their compositional dependence.

Chapter 2

Materials and Methods

2.1 Ti–Ta Alloy

A graded composition rod containing Ti–Ta alloys of 20 wt % Ta through 60 wt % Ta was furnished for study by Dynamet, a subsidiary of Carpenter Technology Corporation. A step composition change of 5 wt % Ta occured every 0.5 inches across the bar. See figure 2.1. Dynamet utilized a proprietary powder metallurgy process to frabricate the rod[3]. Designed specifically to facilitate the production of Ti alloys that contain high refractory metals, such as Ta, Dynamet's CHIP process incorporates a number of techniques that are employed for their ability to overcome the slow diffusivity of such metals[3]. Beginning with high purity, morphology, and particle size distribution controlled titanium and tantalum powders, a powder blend of specified chemistry is fabricated. Successive steps of Cold Isostatic Pressing, vacuum sintering, and Hot Isostatic Pressing are used to produce the fully dense alloy. Final components can undergo secondary metalworking processes like forging or extrusion if further shaping is necessary.

Preliminary testing of the alloys contained in the rod established a working baseline of information on the structure and mechanical properties of each composition. X-ray diffractometry (XRD) was used to determine the crystal structure of each composition. It was found that the system transitioned from predominantly an hcp, α-Ti structure at low wt % Ta to a bcc, β-Ti structure incorporating an orthogonal martensite phase above 40 wt % Ta (figure 2.1). EDX demonstrated that homogeneity of the alloys decreases with increasing wt % Ta, a result that is reasonable given the refractory nature of Ta.

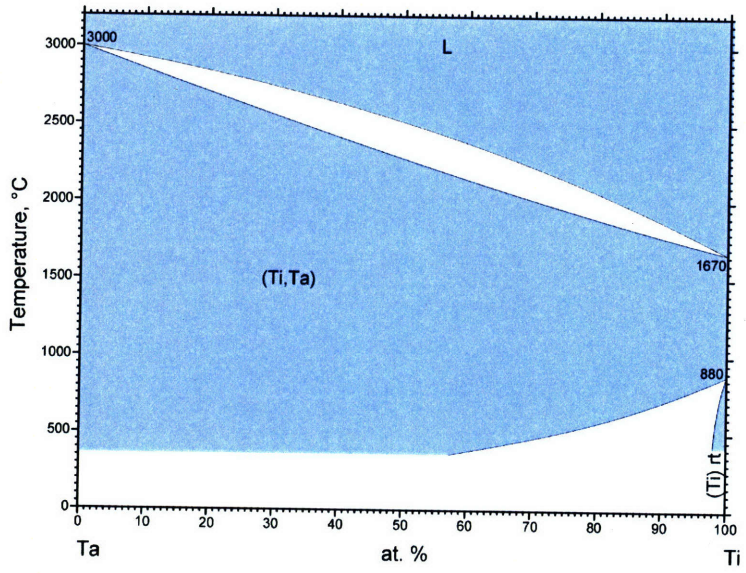

Figure 2-1: Ti–Ta phase diagram. Image courtesy of ASM International and Kaufman et al.

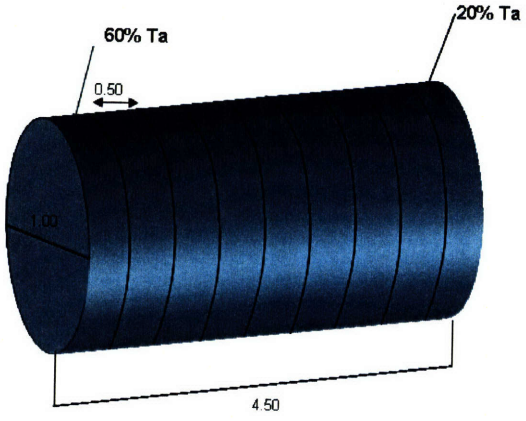

Figure 2-2: Schematic representation of the graded composition bar provided by Dynamet. Length measurements are in inches.

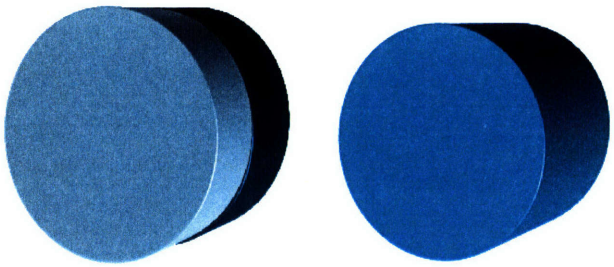

Figure 2-3: Schematic of interfacial (left) and single composition (right) samples.

2.2 Electrical Discharge Machining (EDM)

To gain access to the interface regions, those where a step composition change occurs, the sample was precision machined by EDM. A copper wire Charmilles ROBOFIL 380 EDM cutter was used to make incisions parallel to and on either side of each interface. In this manner, two sets of samples were fabricated: those that contained an interface region and, therefore, incorporated two compositions, and those that, lacking an interface, were comprised of only one composition (see figure 2.2). The former were the only samples utilized in this study.

A second cut was made in those samples that contained an interface region. The purpose of this cut was to, from the cylindrical sample, create a sample with a flat, horizontal surface suitable for imaging in the SEM. As the raw material for these samples, the graded composition bar, was limited and precious, it was necessary to minimize waste and loss. EDM was again utilized for the second incision which was made perpendicular to the interface within the sample (see figure 2.2). The smaller segment of the sample, approximately $\frac{1}{3}$ the height of the uncut sample, was used for all antecedent testing and analysis. Eight samples in total were fabricated.

2.3 Metallographic Specimen Preparation

Each of the eight samples was set into a 1.5 inch diameter Bakelite mount (figure 2.3). Struers Multifast Green was added in the quantity of 1.5 scoops to a Struers Prontopress to create the

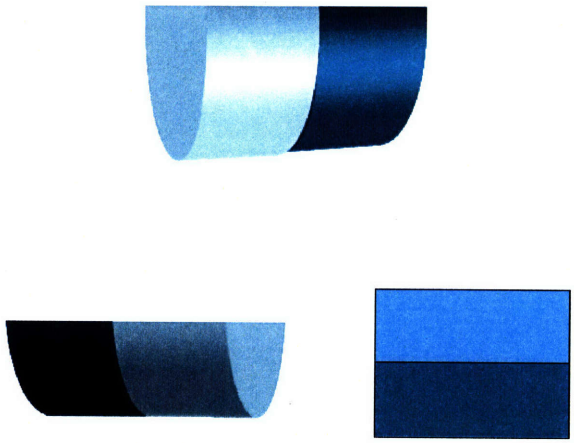

Figure 2-4: Schematic of the unused portion of interfacial sample (top, center), the segment of sample utilized for SEM analysis (lower left), and the top-view of the sample illustrating the position of the interface in the sample (lower right).

Figure 2-5: Schematic of mounted, polished sample.

mount. The heat treatment process involved a four minute ramp up to and a ten minute hold at the maximum temperature of 413 K which was followed by a four minute ramp down or cooling period. A strip grinder was then used to polish the sample to 15 μm surface roughness. A final polish was used to obtain a 6 μm finish. Six μm diamond paste prepared by Heather Lechtman of the Center for Materials Research in Archeology and Buehler Lapping Oil were used on a polishing wheel to complete this final step. In between each polishing step, the sample was cleaned to remove any large particles that could damage the surface as the polish progressed to finer grits. Wetted cotton swabs were used to wash the surface with Ivory soap and deionized, distilled water. Samples were air dried.

2.4 Energy-Dispersive X-Ray (EDX) Analysis

Prior to examination in the SEM, all samples were thoroughly cleaned to remove particulates from the surface. The same method described in section 2.3 was again employed to clean each sample. A JEOL JSM-5910 SEM was used to probe the sample in conjunction with Rontec Quantax Version 1.5 analysis software. Dr. Anthony Garratt-Reed provided training and support for SEM operation.

2.4.1 Operating Parameters

A vacuum of at least 10^{-4} torr in the SEM sample chamber was ensured prior to any SEM analyses. A 25 kV accelerating voltage was used for all experiments. Secondary imaging mode (SEI) was used to bring the sample into focus, establish the working distance, and orient on the sample. A spotsize of approximately 40 was utilized while in SEI.

Following the preliminary focus, the working distance was adjusted to 10 mm and imaging was changed from SEI to backscattering composition mode (BEC). BEC was employed to visually inspect the compositional variation across the surface. As the atomic numbers of Ti and Ta are very different, the two atoms will scatter with different probabilities and, therefore, at different rates[5, 6]. This disparity in scattering rates produces a contrast image where regions of Ti and Ta are visible. Were the sample completely homogeneous, no contrast would be visible as the average value recorded by the collector would be uniform across the surface. Though the runtime software automatically adjusts the spotsize when imaging is changed to BEC it is frequently necessary to fine tune this value. The spotsize should be optimized for high contrast and count rate while avoiding saturation of the collector. The average spotsize value employed while in BEC mode was 48. For higher wt % Ta alloys, the contrast between the Ti and Ta regions is very distinct and visible (figure 2.6). As the quantity of Ta in the alloy decreases, however, the alloys become more homogeneous such that

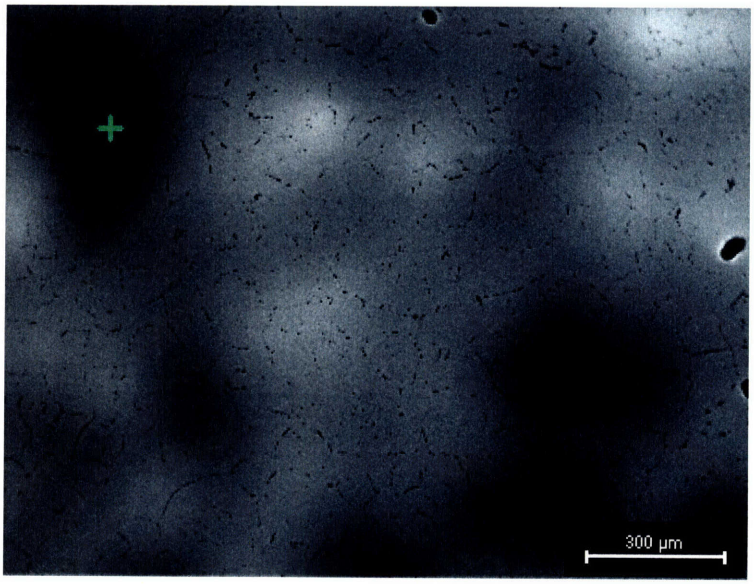

Figure 2-6: BEC image of 55 wt % Ta. Whiter areas correpond to Ta-rich regions while darker areas are Ti-rich.

regions of Ti and Ta are difficult to differentiate (figure 2.7). Contrast values, for this reason, were adjusted to maximize visibility of the compositional variation while maintaining image quality and resolution. Higher contrast was used for lower weight fraction Ta alloys.

2.4.2 Diffusion Couples

2.4.2.1 Location of the Interface

The graded composition bar provided a unique opportunity to examine interdiffusivity as diffusion couples between neighboring compositions were inherent in the samples. With interest in utilizing the interface of step composition change between two regions of nominally uniform composition as a diffusion couple, it was necessary to locate and assess the quality of the interfaces. BEC imaging allowed for visual indentification of the interface. As whiter regions of the images corresponded to Ta-rich areas, the interface was identified by inspection of where a discernable difference in the average shade of the sample surface. Due to the manner of alloy fabrication, the interface formed an approximately straight line across the area imaged. Visual detection of the interface at lower wt % Ta was aided by the overall greater homogeneity of the samples. Visual detection became increasingly difficult with increasing wt % Ta. Composition fluctuations were larger for higher wt % Ta such that the 5 wt % difference in composition across the interface was not as significant. Interfaces for high wt % Ta alloys were hazy and ill-defined. The difference between even the definition of the 40 to 45 wt % Ta interface and the 50 to 55 wt % Ta interface is, as seen in figures 2.8 and 2.9, significant.

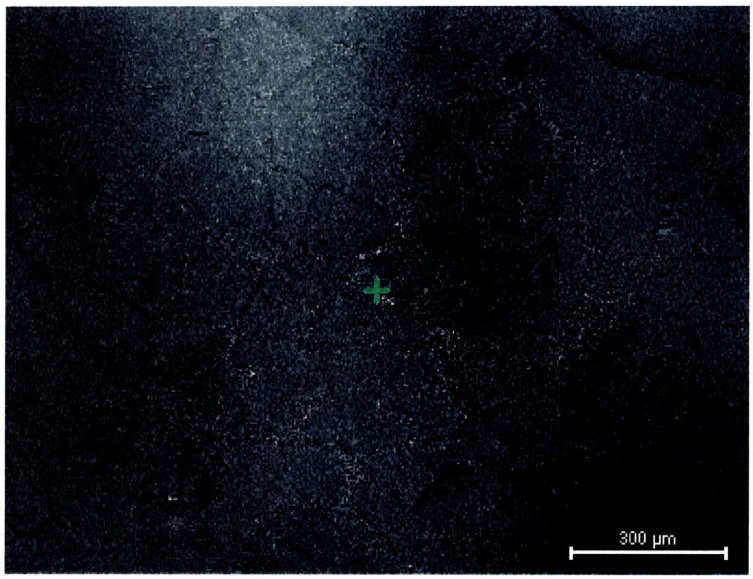

Figure 2-7: BEC image of 20 wt % Ta. Whiter areas correpond to Ta-rich regions while darker areas are Ti-rich.

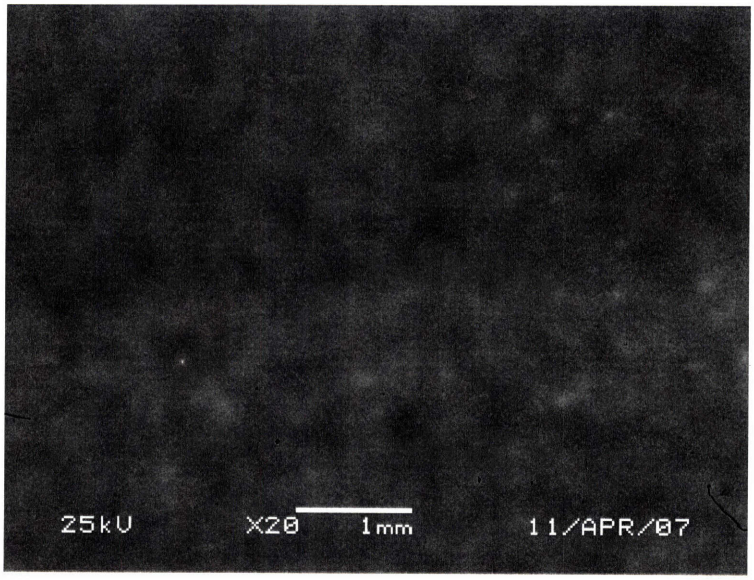

Figure 2-8: BEC image of interface between 40 and 45 wt % Ta. Whiter areas correpond to Ta-rich regions while darker areas are Ti-rich.

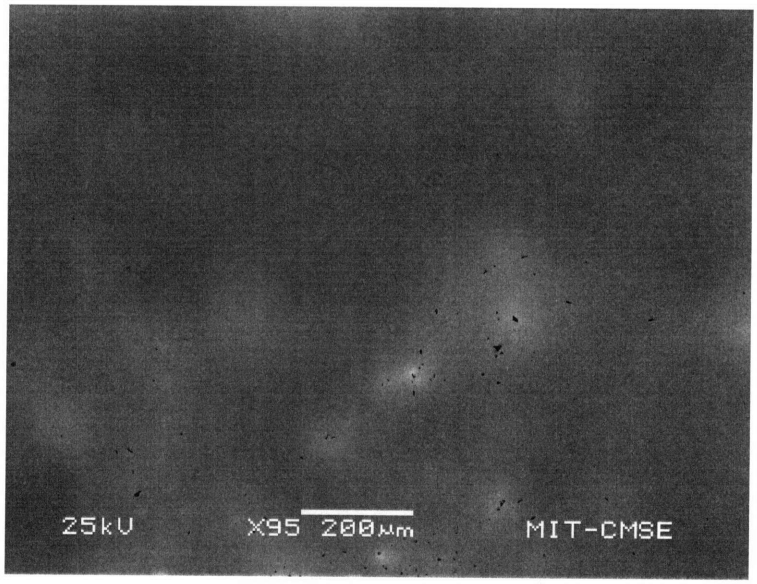

Figure 2-9: BEC image of interface between 50 and 55 wt % Ta. Whiter areas correpond to Ta-rich regions while darker areas are Ti-rich.

To confirm the presence of an interface, EDX was used to collect an average value of composition across the scan area in which an interface was visually indentified. The presence of an interface was confirmed if a composition value that was the average of the two extremes was obtained (e.g. a value of 42.5 wt % Ta for the interface between 40 and 45 wt % Ta).

2.4.2.2 Micro versus Macro Diffusion Couples

Study of interdiffusion requires the clear definition of a diffusion couple. The images and data indicating the poor definition of interfaces between higher wt % Ta alloys undermined the feasibility of their use as a diffusion couple. EDX of several points on either side of the interface revealed that composition fluctuations within a region of uniform average composition were greater than the step change in composition across the interface. The decreased homogeneity for increasing wt % Ta was also evident in the more irregular interfacial boundaries seen at these compositions. Refer to figure 2.9. In light of these considerations, the interfaces did not serve as the diffusion couples for the analysis.

Large composition fluctuations had precluded use of the interface as a diffusion couple. This same variance, however, enabled consideration of diffusion couples on a smaller length scale. The candidate for these micro diffusion couples were the inter-region fluctuations. Dynamet had prepared each composition within the graded rod by blending pure Ti and pure Ta powders in the desired proportions[3]. Though fine details of the processing method were not disclosed, this initial condition

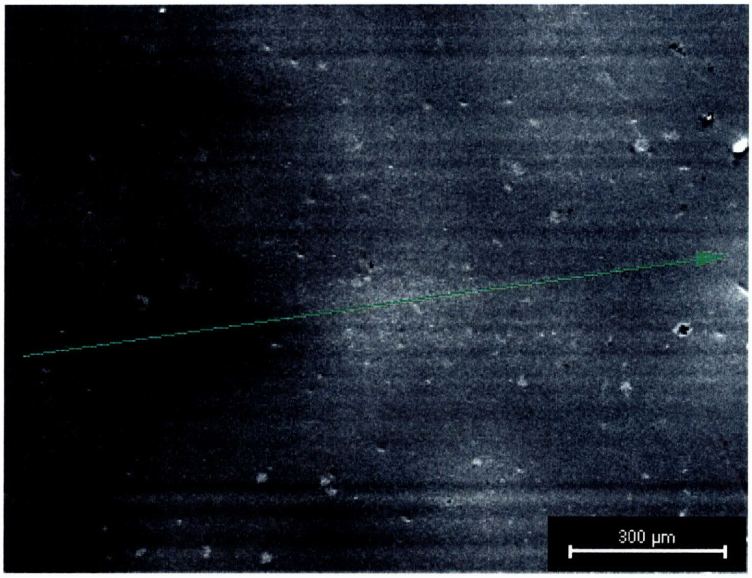

Figure 2-10: Linescan vector for a 40 wt % Ta sample. The arrow indicates the path of the linescan. White areas are Ta-rich while dark areas are Ta-poor. The linescan traverses at least one of each region.

enables consideration of the junction between two powder particles as a diffusion couple.

2.4.2.3 Linescans of Composition

EDX was utilized to conduct linescans of and obtain composition profiles for the micro diffusion couples. All linescans were conducted parallel to the interface to ensure that only fluctuations within a region of nominally uniform composition were measured. Confirmation of a region's average composition was provided by an EDX measurement of composition across that area. This measurement was indicative of the average composition in that region. If the measured value did not correlate well with the known composition of that region, no linescans were obtained from that area. Optimal linescan vectors were determined through visual inspection of the surface. A trajectory that crossed at least one Ta-rich and one Ti-rich region was necessary for computational modeling. See figure 2.10. At least three linescans were collected per composition. Linescans were gathered from a minimum of two distinct regions of the sample for a given composition. To aid analysis of the linescan data, composition values were sampled for at least one point on each linescan.

Measures were taken to ensure that high precision values of composition were gathered from the linescans. The measurement error for an SEM is $2\sqrt{\#counts}$[6]. To get 1 % error in a measurement it is necessary to collect 10,000 counts. The JEOL SEM utilized in this research is capable of gathering 150,000 counts per second (cps). It is important to note that the number of count requirement is per

probed piece of material and per site probed. As linescans gather composition values across a narrow but long strip of material, the number of cps supplied by the beam are spread across this region. A sufficient number of counts in each experiment was ensured by collecting data for a minimum of 210 seconds at a count rate no less than 4.5 kcps.

2.4.3 Conversion of EDX data from counts to composition

The native output of EDX linescan data is cps as a function of position. For analysis and computational modeling, the raw linescan data required conversion to wt % Ta as a function of position on the sample surface. A direct conversion of counts to composition is prohibited by the fact that Ti and Ta differ in their probability of emission. To account for the disparity in probabilities, a constant weighting factor must be determined for each data set. For a given composition with a weight fraction of Ti, C_a, and weight fraction of Ta, C_b, it can be shown that

$$C_B = \frac{N_B}{N_B + N_A \cdot K_{AB}} \text{ and } C_A = \frac{N_A \cdot K_{AB}}{N_B + N_A \cdot K_{AB}}$$

where N_A and N_B are the counts of Ti and Ta, respectively, and K_{AB} is the probabilistic weighting factor. Values for K_{AB} were derived from experimental data. The average composition of each area across which a linescan had been taken was determined prior to the collection of any data. As linescan lengths were approximately equal to the length of the sampled area, the average composition value across the linescan should be equivalent to that of the area. Derivation of K_{AB} values was then enabled by setting the C value to that of the measured average composition for that area, N to the average number of counts, and algebraically solving for K_{AB}. This calculation was performed for each individual linescan to ensure the highest precision results.

2.4.4 Analysis of EDX composition data

Plots of converted EDX linescan data reveal small oscillations across the length of the scan. See figure 2.11. These small fluctuations are within the limits of machine noise such that they are not significant features of the data[5, 6]. A moving average filter was applied to the data to reduce these oscillations and clarify the true features of the data. See figure 2.12. A moving average of three values was typical of the data. Increased noise in the data was observed for higher wt % Ta samples. The filter was adjusted when necessary to accomodate the increased fluctuations. Filters utilizing odd numbers were preferential as they provided an equal number of points above and below a value. In this way a true average for each data point was obtained without weighting lower or higher values

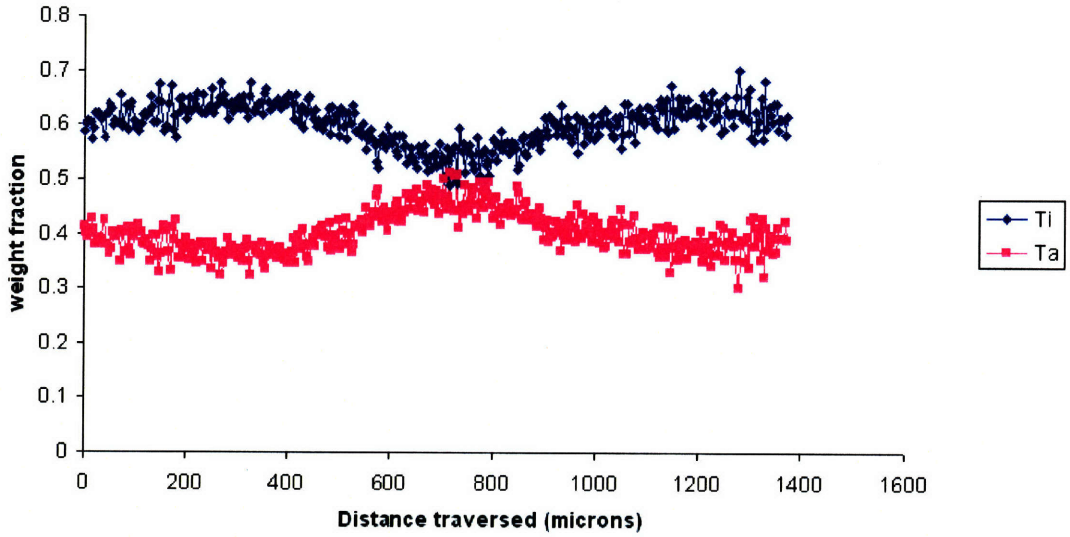

Figure 2-11: Unfiltered linescan of composition for 40 wt % Ta.

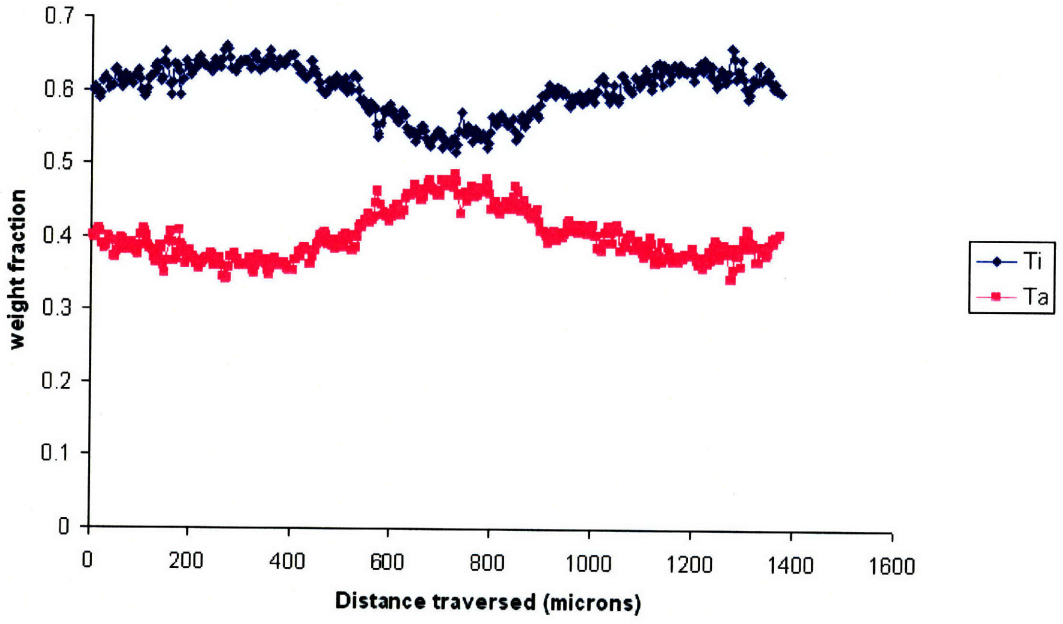

Figure 2-12: Filtered linescan of composition for 40 wt % Ta.

unequally. Care was taken in application of the filter to avoid averaging out features of the data. Visual inspection of BEC images of linescans provided confirmation of significant features of the data.

Chapter 3

Results and Discussion

3.1 Computational Model

A linearized version of Fick's Second Law was used to model the linescan data. Fick's Second Law states that, for diffusion in one dimension,

$$\frac{\delta c}{\delta t} = -\frac{\delta J}{\delta x} = -\frac{\delta}{\delta x}\left(-D\frac{\delta c}{\delta x}\right) = D\frac{\delta^2 c}{\delta x^2}$$

where J is diffusion flux in $\frac{mol}{m^2 \cdot s}$, D is the diffusion coefficient or diffusivity in $\frac{m}{s^2}$, c is the concentration in $\frac{mol}{m^3}$, and $x$is the position in m[1, 4]. Fick's Second Law was linearized by assuming that D was independent of concentration. The separation of variables method was used to solve the linearized version of Fick's Second Law and obtain diffusivity values. A periodic system with "rectangle wave" initial conditions and no volume change during diffusion was assumed. The general form of the solution is

$$c(x,t) = \bar{c} + \sum_{n=1}^{\infty}\left[b_n \cdot \cos\frac{n\cdot\pi\cdot x}{L}\right] \cdot \exp\left(\frac{n^2\cdot\pi^2}{L^2}\cdot Dt\right)$$

where $\bar{c}$ is the composition at long times, L is the length of the diffusion couple in m, x is the distance traversed along the diffusion couple in m, n is the summation index, and t is time in s. The exact solution was approximated by limiting the summation from $n = 0$ to $n = 200$. This approximation is valid given that long diffusion times and shallow concentration gradients were considered by this model. The term b_n carries the initial conditions and is given by

$$b_n = \frac{2}{L}\int_0^{x'} \cos\frac{n\cdot\pi\cdot x}{L}dx$$

where x' denotes the length at which the interface between pure Ta and Ti regions lies for $t = 0$. Values of x' vary with the volume fraction of Ta in each sample. A unique value of x' was, therefore, computed for each dataset. The value of x' in m was calculated by

$$x' = \frac{C_B \cdot \rho_{Ti} \cdot L}{((1-C_b) \cdot \rho_{Ta} + C_b \cdot \rho_{Ti}}$$

where $\rho_{Ti}$and ρ_{Ta} are the densities of Ti and Ta, respectively. Density was assumed to be independent of composition. All of the variables in the four antecedent equations are either constants or are derived from the data such that D remains a fitting parameter.

3.2 Model of Experimental Data

All of the Ti–Ta samples underwent the same heat treatment for 24 hours at 1473 K[3]. This uniform processing history controlled for all variables save one in the computational model. The value of interdiffusivity was used to fit the model curve to parameters derived from experimental data. Interdiffusion of two blocks of material has the inital condition of a step composition change from a weight fraction of one to a weight fraction of zero across the interface between the two blocks. If the blocks are allowed heated and allowed to interdiffuse, the sample will approach a uniform and homogeneous composition at long times. Models of this behavior produce composition profiles where composition is plotted against distance along the diffusion couple. Evolution from the intial condition results in a change in the amplitude of the composition profile. Composition profiles are then the model's corollary of the experimental linescan profiles. Given that the amplitude of a composition profile reflects the influences of time and the diffusion coefficient, the D value was adjusted to ensure an optimal fit of the curve amplitude. Curve amplitude was derived by first collecting a composition and position for both a Ta-rich and Ti-rich region in the experimental data. The composition values at these extrema were subtracted to derive the curve amplitude. D was adjusted until the amplitude of the model curve matches that of the experimental. See figures 3.2 and 2.12. This value of D is taken to be the interdiffusivity for a given linescan at a specific wt % Ta. See figure 3.2.

3.3 Error Analysis

Multiple linescans were gathered at each composition. A unique interdiffusivity value was comuted for each linescan such that multiple interdiffusivity values were obtained for each composition. The

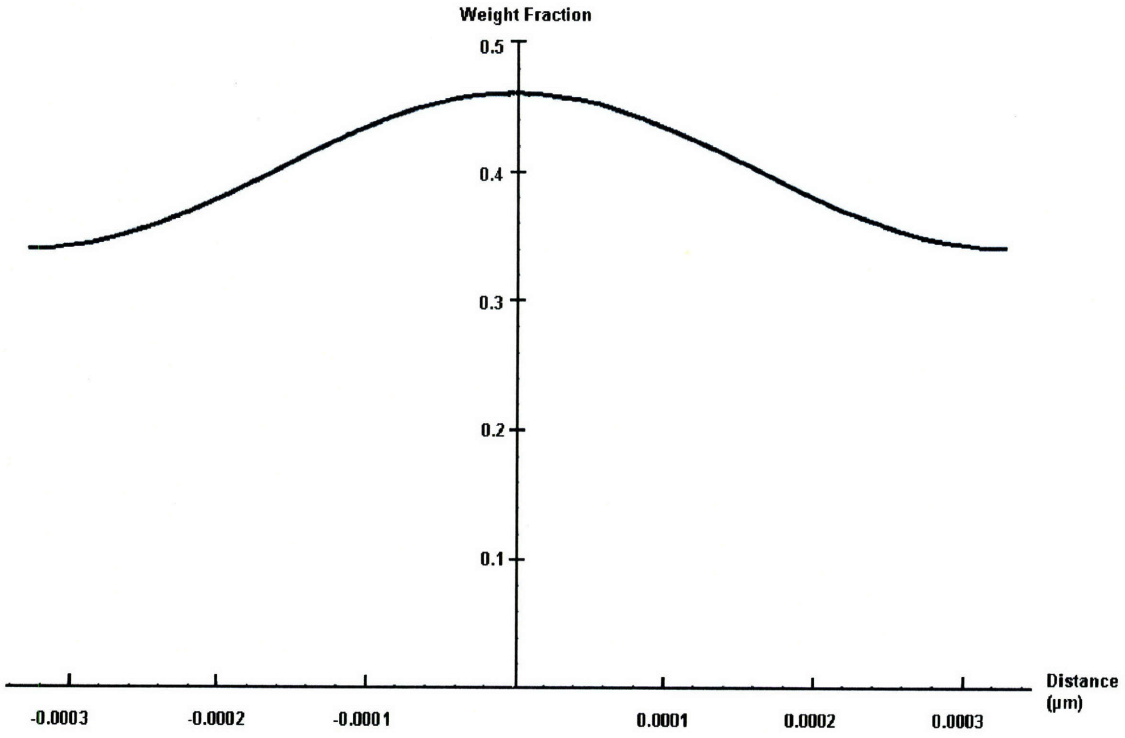

Figure 3-1: Computational model curve for a single period in a 40 wt % Ta alloy.

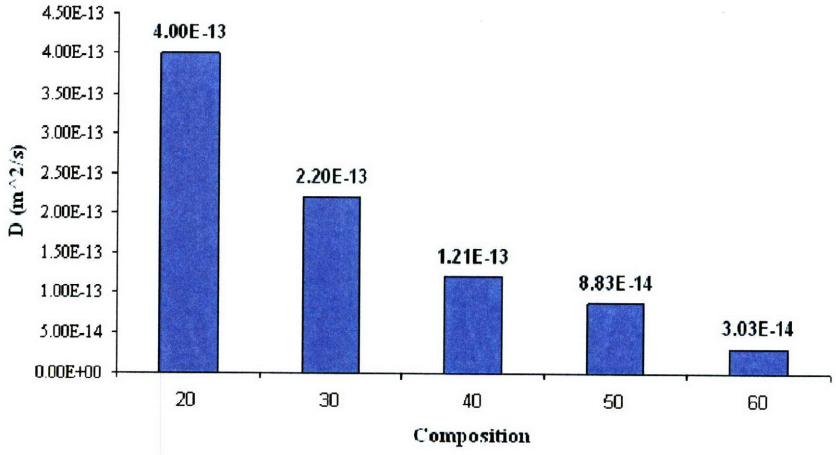

Figure 3-2: Interdiffusivity values.

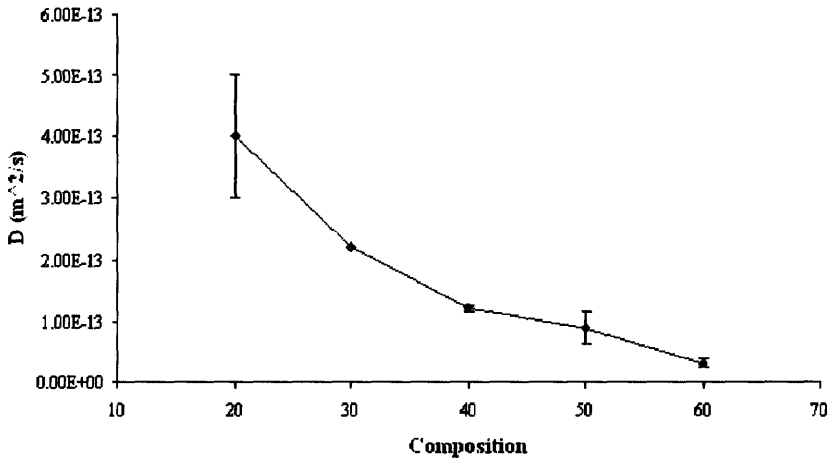

Figure 3-3: Standard deviation of interdiffusivity values.

average interdiffusivity value and standard deviation were computed from these data (figure 3.3). Though more data would be necessary to determine a conclusive trend, it appears that error is inversely proportional to wt % Ta. The increased error at these lower Ta compositions is a result of their greater homogeneity. Fluctuations in composition were less pronounced for these lower Ta alloys. As amplitude values were determined by inspection of linescan data, a more pronounced fluctuation would allow for greater accuracy in determination of maximum and minimum composition values. Maxima and minima were used to extract both the amplitude of the curves and the length of the diffusion couple. Since linescan data was fit by matching these two key parameters, error in the amplitude of the curves and the length of the diffusion couple would propagate through to the interdiffusivity values. Lower wt % Ta alloys, with greater error in the extraction of amplitude and diffusion couple length, then have greater error in their interdiffusivity values.

Chapter 4

Conclusions and Future Work

EDX was utilized to gather linear compositional traces. Each trace was conducted parallel to the interface of step composition change across micro diffusion couples. A linearized Fick's Second Law equation was used to computationally model the data. Interdiffusivity values were found to range from $4.0 \cdot 10^{-13} \frac{m^2}{s}$ for 20 wt % Ta to $3.0 \cdot 10^{-14} \frac{m^2}{s}$ for 60 wt % Ta. The interdiffusion coefficient was seen to systematically vary with Ta composition such that interdiffusivity decreased with increasing wt % Ta. Qualitative confirmation of this result was evident in BEC images of the samples where inhomogeneity of the sample increased with wt % Ta.

The results of this study suggest several possible directions for future work. Derivation of increasingly precise values of the interdiffusivity would benefit development of appropriate processing pathways for Ti–Ta alloys. Computation models utilized in this work derived interdiffusivity values by leaving it as fitting parameter for experimental data. The amplitude and period of the oscillation was the main parameter fit by the model. Extraction of amplitude values from experimental data relied on a few oscillations at most. Were longer linescans conducted, the amplitude values from several oscillations could be recorded. A Fourier Transform of this data could then reveal the dominant oscillation. Greater precision in computation of the amplitude values would enable greater precision in computation of interdiffusivity values.

The computational model in this study linearized Fick's Second Law by treating interdiffusivity as independent of composition. The validity of this assumption is undermined by the observation of a distinct, systematic variation in interdiffusivity values with composition. To examine the effects of this assumption on interdiffusivity values, a study involving treatment of data with the full, non-linear Fick's Second Law equation could be performed.

Another avenue for further research is the investigation of macro diffusion couples of Ti–Ta alloys. Sample inhomogeneity increased with wt % Ta. Fluctuations in composition within a region, therefore, surpassed in magnitude the 5 wt % step composition change between regions. Use of the interfacial region as diffusion couple was then pre-empted. Additional homogenization treatments to remove the small scale variation within regions would enable use of the interface as a macro diffusion couple.

Bibliography

[1] Robert W. Balluffi, Samuel M. Allen, and W. Craig Carter. *Kinetics of Materials.* John Wiley and Sons, 2005.

[2] James A. Davidson and Paul Kovacs. Biocompatible low modulus titanium alloy for medical implants. Patent, January 1991.

[3] Dynamet. Sbir phase one research plan. December 2006.

[4] C. Henry Edwards and David E. Penny. *Elementary Differential Equations with Boundary Value Problems.* Prentice-Hall, Inc., 2000.

[5] Barbara L. Gabriel. *SEM: A User's Manual for Materials Science.* American Society for Metals, 1985.

[6] A.J Garratt-Reed and D.C. Bell. *Energy Dispersive X-Ray Analysis in the Electron Microscope.* BIOS Scientific Publishers Limited, 2003.

[7] K.D. Hunt, V. Dean O'Loughlin, D.W. Fitting, and L. Adler. Ultrasonic determination of the elastic modulus of human cortical bone. *Medical and Biological Engineering and Computing*, 36:51–56, 1998.

[8] Michail Yu Kollerov, Alexander A. Ilyin, and Dmitry Yu Makarenkov. Martensitic transformations and shape memory effect in titanium alloys. In *Titanium: Science and Technology.* 1995.

[9] R.W. Margevicius and J.D. Cotton. Stress-assisted transformation in ti-60 wt pct ta alloys. *Metallurgical and Materials Transactions*, 29A:139–147, 1998.

[10] Jeff Perkins, editor. *Shape Memory Effects in Alloys.* Plenum Press, 1975.

[11] D.A. Porter and K.E. Easterling. *Phase Transformations in Metals and Alloys.* Taylor and Francis Group, 2004.

[12] Robert E. Reed-Hill and Reza Abbaschian. *Physical Metallurgy Principals.* PWS Publishing, third edition, 1994.

[13] Paul Shewmon. *Diffusion in Solids.* Minerals, Metals, and Materials Society Press, 1989.

[14] D. Starosvetsky and I. Gotman. Corrosion behavior of titanium nitride coated ni-ti shape memory surgical alloy. *Biomaterials*, 22:1853–1859, 2001.

[15] Richard Tilley. *Understanding Solids: The Science of Materials.* John Wiley and Sons, 2004.